HHS Public Access

Author manuscript

Oncogene. Author manuscript; available in PMC 2020 February 12.

Published in final edited form as:

Oncogene. 2019 October ; 38(43): 6913–6925. doi:10.1038/s41388-019-0941-0.

Dynamic interactions between the extracellular matrix and estrogen activity in progression of ER+ breast cancer

Fatou Jallow[*,1,2], **Kathleen A. O'Leary**[*,1], **Debra E. Rugowski**[1], **Jorge F. Guerrero**[3], **Suzanne M. Ponik**[3,4], **Linda A. Schuler**[1,4,**]

[1]Department of Comparative Biosciences, University of Wisconsin-Madison, Madison, WI

[2]Endocrinology-Reproductive Physiology Program, University of Wisconsin-Madison, Madison, WI

[3]Department of Cell and Regenerative Biology, University of Wisconsin-Madison, Madison, WI

[4]University of Wisconsin Carbone Cancer Center, University of Wisconsin-Madison, Madison, WI

Abstract

Metastatic, anti-estrogen resistant estrogen receptor α positive (ER+) breast cancer is the leading cause of breast cancer deaths in U.S. women. While studies have demonstrated the importance of the stromal tumor microenvironment in cancer progression and therapeutic responses, effects on the responses of ER+ cancers to estrogen and anti-estrogens are poorly understood, particularly in the complex *in vivo* environment. In this study, we used an estrogen responsive syngeneic mouse model to interrogate how a COL1A1-enriched fibrotic ECM modulates integrated hormonal responses in cancer progression. We orthotopically transplanted the ER+ TC11 cell line into wild-type (WT) or collagen-dense (*Col1a1*$^{tm1Jae/+}$, mCol1a1) syngeneic FVB/N female mice. Once tumors were established, recipients were supplemented with 17β-estradiol (E2), tamoxifen, or left untreated. Although the dense/stiff environment in mCol1a1 recipients did not alter the rate of E2-induced proliferation of the primary tumor, it fostered the agonist activity of tamoxifen to increase proliferation and AP-1 activity. Manipulation of estrogen activity did not alter the incidence of lung lesions in either WT or mCol1a1 hosts. However, the mCol1a1 environment enabled tamoxifen-stimulated growth of pulmonary metastases and further fueled estrogen-driven growth. Moreover, E2 remodeled peritumoral ECM architecture in WT animals, modifying alignment of collagen fibers and altering synthesis of ECM components associated with increased alignment and stiffness, and increasing FN1 and POSTN expression in the pulmonary metastatic niche. These studies demonstrate dynamic interactions between ECM properties and estrogen activity in progression of ER+ breast cancer, and support the need for therapeutics that target both ER and the tumor microenvironment.

**To whom correspondence may be addressed: linda.schuler@wisc.edu.
*These authors contributed equally to this work.

Supplementary information is available at Oncogene's website.

Competing Interests

The authors declare that they have no competing interests.

Introduction

The extracellular matrix (ECM) is increasingly recognized as a critical component of the tumor microenvironment, which can profoundly influence tumor behavior, metastasis and patient survival [1–4]. As solid cancers grow, collagen deposition increases around the tumor [5, 6]. For estrogen receptor alpha positive (ER+) breast cancers, which constitute 75% of breast cancer cases in the United States [7], collagen structure is an independent prognostic indicator of reduced disease-free survival [8]. Estrogen is a major mitogenic driver of many ER+ cancers, and anti-estrogens are the cornerstone of the therapeutic strategies. While most patients respond to these treatments, a substantial number are initially resistant or become resistant, especially in the metastatic setting [9, 10]. Indeed, advanced therapy resistant ER+ disease accounts for the majority of breast cancer mortality [11]. How the characteristics of the ECM influence the outcome of estrogen signals, and equally importantly, the responses to anti-estrogens, is poorly understood. Moreover, although the contribution of hormones to mammographic density, including stromal density, is widely appreciated [12, 13], how estrogen exposure prior to diagnosis influences the peritumoral ECM has not been examined.

We demonstrated that ECM density and stiffness can alter the repertoire and outcomes of hormonal signals to ER+ human breast cancer cells *in vitro* [14–16]. Varying matrix density/stiffness does not affect the magnitude of 17β-estradiol (E2)-induced proliferation of cells grown in 3-D collagen I matrices. However, in stiff matrices, E2-induced growth is less sensitive to inhibition by tamoxifen, a selective estrogen receptor modulator (SERM), which is the first line treatment for premenopausal women with ER+ breast cancer [17]. Moreover, ECM properties strongly modulate the estrogen responses of endogenous target genes, indicating that matrix properties can influence the E2-regulated transcriptome [15]. Further, stiff/dense COL1A1 matrices enable hormone-induced invasion, which is not evident in compliant environments [15]. Conversely, hormones also modulate the organization of collagen fibers in dense/stiff 3-D collagen I matrices [15].These studies demonstrate reciprocal interactions between matrix properties and hormone signals in well-characterized breast cancer cell lines in defined COL1A1-enriched *in vitro* systems.

Despite the wealth of knowledge accrued in *in vitro* models, the interplay between ECM characteristics and estrogen/anti-estrogen actions in a dynamic *in vivo* environment is poorly understood. The paucity of immunocompetent models of ER+ aggressive disease has limited our ability to probe the effects on behavior of primary ER+ tumors and disseminated tumor cells. Here we utilized a hormonally-induced mouse model of ER+ breast cancer, which displays many characteristics of aggressive luminal B clinical cancers [18–20]. We used an ER+ cell line derived from these estrogen responsive metastatic cancers , in conjunction with a model of elevated collagen deposition, *Col1a1*$^{tm1Jae/+}$ (mCol1a1) [21], to mimic the desmoplasia surrounding growing tumors. A point mutation in the *Col1a1* gene in these mice renders the protein collagenase-insensitive, and the consequent reduced turnover leads to accumulation of COL1A1, increasing ECM density and stiffness. We orthotopically transplanted an ER+ tumor cell line into syngeneic wildtype (WT) or mCol1a1 female mice, and once tumors were established, mice were treated with supplemental E2 or tamoxifen. The dense/stiff environment in mCol1a1 recipients did not alter the rate of E2-induced

proliferation of the primary tumor, but permitted tamoxifen to robustly increase tumor growth, associated with increased activating protein 1 (AP-1) activity. The collagen I-dense environment increased the number of lung metastases, but estrogen activity did not further alter the frequency. However, E2 increased the size of the lung lesions in WT recipients, which was further enhanced in mCol1a1 recipients. Moreover, E2 altered the orientation and synthesis of ECM components in the tumor environment in WT animals. Together, these studies demonstrate the power of collagen density to modulate hormone responses, and reciprocally, the ability of estrogen to remodel the ECM. Understanding this dynamic interplay between hormones and the tumor microenvironment is essential to understand estrogen and tamoxifen actions in aggressive ER+ breast cancers prior to diagnosis and initiation of treatment.

Results

Primary tumors are estrogen responsive, and both E2 and tamoxifen increase tumor growth in mCol1a1 recipients

To investigate the effect of a collagen I-rich environment on the responses of ER+ mammary tumors to E2 and the SERM, tamoxifen, we utilized a murine ER+ mammary tumor cell line derived from an ER+ adenocarcinoma that spontaneously developed in a NRL-PRL female [19]. 10 000 TC11 cells were orthotopically transplanted into syngeneic WT and mCol1a1 female mice. When tumors reached 150 mm^3, mice were implanted with pellets releasing E2 or tamoxifen citrate, or left untreated (Fig. 1a). Primary tumors in untreated WT recipients grew slightly faster than in mCol1a1 hosts (Fig. 1b, interaction between genotypes, p=0.03). However, the collagen environment did not alter the spindle cell morphology, or expression of ER or progesterone receptor (Fig. 1c, i-iv; Suppl. Fig. 1a). Staining of fibrillar collagens with picrosirius red revealed substantial collagen deposition, particularly around the tumor boundary in mCol1a1 compared to WT recipients (Fig. 1c, v-vi), as well as increased COL1A1 expression within the tumor (Suppl. Fig. 1a).

E2 robustly increased tumor growth compared to untreated females in both genotypes (Fig. 1d,e). In WT hosts, tamoxifen did not alter tumor growth, indicating that these tumors are not markedly dependent on estrogenic ligands in this setting. However, in mCol1a1 females, tamoxifen fueled tumor growth (Fig. 1e). Ki-67 staining of end stage tumors reflected these findings, indicating that tamoxifen promotes tumor cell proliferation in the mCol1a1 environment (Fig. 1f). Regardless of genotype, estrogen activity did not alter tumor morphology (Suppl. Fig. 1b).

Estrogen activity does not influence the number of lung metastases, but E2 enlarges lesions in both genotypes and tamoxifen increases lesion area in mCol1a1recipients

One of the common sites of metastasis of luminal B breast cancers is the lung [22–24], and metastatic dissemination by endogenous routes to this site is mimicked by tumors in the NRL-PRL model [18]. After orthotopic transplantation of TC11 tumor cells, pulmonary lesions were readily histologically detectable in both recipient genotypes in all treatment groups at end stage (Fig. 2a, i). Like the primary tumors, lung lesions in both WT and mCol1a1 recipients expressed ER (Fig. 2a, ii). mCol1a1 recipients developed significantly

more lesions than WT recipients, similar to reports of other tumor cell sources in the mCol1a1 model [25–27]. Manipulation of estrogen activity did not alter the number of lung metastases that developed in either WT or mCol1a1 recipients (Fig. 2a, iii), indicating that once tumors were established, it has no net effect on the sum of the processes that result in successful initiation of pulmonary lesions. However, E2 significantly increased the size of the metastases in recipients of both genotypes, and further enlarged lung lesions in mCol1a1 recipients compared to similarly treated WT females (Fig. 2a, iv). In WT females treated with tamoxifen, lung lesions remained small, as in untreated animals. However, in mCol1a1 recipients, tamoxifen also significantly enlarged metastases compared to similarly treated WT animals, although not to the extent of E2 (Fig. 2a, iv). These results reflect the culmination of multiple events that result in endogenous metastasis. In order to distinguish possible differences in the lung environments of WT and mCol1a1 females from systemic consequences of long term interactions of ECM properties and the primary tumor that might contribute to these findings, we injected 10 000 TC11 cells intravenously via the tail vein. As shown in Fig. 2b, i-ii, fewer metastases were established by this delivery method than by endogenous metastatic routes, but the sizes of lesions were similar to those originating from dissemination of orthotopic tumors. However, no significant differences were observed in the number or size of these lesions between WT and mCol1a1 females, suggesting that the lungs of these genotypes do not exhibit large inherent differences.

Collagen I-rich environments activate signaling cascades

Multiple studies have demonstrated the ability of the surrounding ECM to alter patterns of activated signals in tumor cells, including focal adhesion kinase, MAP kinases, and the PI3K-AKT cascade [1, 3, 26–28]. Primary tumors in untreated mCol1a1 recipients in this study exhibited higher levels of pERK1/2 and trended to higher levels of pAKT, compared to those in WT hosts (Fig. 3). PAK1 is activated by the PI3K/PDK1 pathway, and cooperates with AKT and activates MAP kinases to promote oncogenic processes. This kinase, which is overexpressed in some breast cancers [29–31], was also expressed at significantly elevated levels in primary tumors in mCol1a1 recipients (Fig. 3). These ECM-augmented kinase cascades would influence multiple transcriptional regulators with potential impact on ER signals.

Collagen I-rich environments increase tamoxifen-induced AP-1 activity

AP-1 activity is implicated in tamoxifen resistance in preclinical models and some studies of patient tumors [32–38]. In light of the ability of activated ER to signal by “tethering” to these transcription factors [39–41], we evaluated effects of the ECM environment on E2 and tamoxifen signals via AP-1 elements. Initially, we examined expression of c-JUN, a component of AP-1 dimers [42, 43]. The collagen I-dense environment was sufficient to increase c-JUN positive cells in primary tumors in the absence of any other treatment (Fig. 4a, b). As predicted from its ability to activate this complex, E2 significantly increased the proportion of tumor cells expressing c-JUN to a similar level in WT and mCol1a1 female recipients. Tamoxifen was able to slightly but significantly increase nuclear c-JUN in WT recipients, but further elevated its expression to the E2-induced level in mCol1a1 recipients. To confirm the increased AP-1 activity predicted by the elevated c-JUN expression, we examined transcripts for well characterized AP-1 target genes [43]. As predicted, transcripts

for cyclin D1 (CCDN1), MMP3, and FOSL1, another AP-1 protein which is positively regulated by AP-1 activity [44], followed a similar pattern (Fig. 4c, i).

In contrast, the ability of E2/ tamoxifen to regulate expression of target genes known to be dependent on an estrogen response element (ERE; *Greb1, Pgr, Stat5a*) was not affected by the mCol1a1 environment (Fig. 4c, ii). Consistently, the responses of STAT5A protein expression followed a similar pattern (Fig. 4d, e). Together, these data indicate that the mCol1a1 environment increases the ability of tamoxifen to activate some, but not all, ER signals.

Estrogen activity modulates components of the ECM in the tumor microenvironment

The studies above demonstrate that the increased ECM density/ stiffness of the mCol1a1 environment permits tamoxifen to drive growth of the primary tumor, and enables both E2 and tamoxifen to further promote growth of pulmonary metastatic lesions. These findings raise the reciprocal question: do these ER ligands alter the peritumoral ECM in the wildtype environment in the absence of this collagen I mutation? Any evidence for bidirectional activity is critical to understand the multiple mechanisms by which estrogen activity may affect undiagnosed cancers. We began by investigating the effect of estrogen activity on ECM architecture in the WT collagen environment. Tumor progression is marked by modification of the ECM structure, including increased deposition and reorganization of collagen fibers. As tumorigenesis proceeds, collagen fibers at the tumor-stromal boundary no longer appear loosely associated (tumor-associated collagen signature-1; TACS-1), and become straighter and more parallel to one another (TACS-2). With additional remodeling, some fibers reorient, aligning perpendicularly to the tumor boundary (TACS-3) [45], and forming tracks for tumor cell invasion [1, 46]. TACS-3 is an indicator of poor prognosis, particularly for ER+ breast cancer [8]. Analysis of picrosirius red-stained fibrillar collagens in the primary tumor microenvironment in WT mice revealed that estrogen activity did not significantly alter the length, diameter or density of the peritumoral collagen fibrils (data not shown). However, the collagen fibers surrounding E2-supplemented tumors were oriented with a significant increase in angle relative to the tumor boundary compared to control or tamoxifen-treated hosts (Fig. 5a, b). In order to further understand effects of estrogen activity on ECM architecture, we examined transcripts for ECM components which have been associated with altered collagen structure or properties [47–49]. The E2-induced ECM reorganization was accompanied by increased transcripts for COL1A1, and several matricellular proteins, including TNC, FN1 and POSTN. In addition, transcripts for the cross-linking enzyme, LOX, and factors regulating TGFβ were upregulated. Taken together these changes predict E2-increased ECM remodeling (Fig. 5c, i-iv). E2-induced FN1 protein expression in primary tumors was confirmed by immunofluorescence (Suppl. Fig. 2). As shown in Fig. 2a, iv, supplementation with E2 increased the size of the pulmonary metastases. In order to determine if this was associated with altered expression of ECM components at these distant lesions, we examined FN1 and POSTN, which have been associated with pulmonary metastases [50, 51], by immunofluorescence. As shown in Fig. 5d, e, E2 increased expression of both proteins.

Discussion

Accumulating studies have demonstrated the importance of the stromal tumor microenvironment in cancer progression and therapeutic responses. While clinical and experimental evidence indicate that stiff, aligned collagen-I environments increase breast cancer aggression [3, 8, 26, 28, 45, 52, 53], the effects of this environment on the responses of ER+ cancers *in vivo* to estrogen and anti-estrogens are poorly understood. In this study, we used an estrogen responsive syngeneic mouse mammary tumor model which develops endogenous pulmonary metastases to interrogate how a COL1A1-enriched fibrotic ECM modulates integrated hormonal responses in cancer progression. We demonstrated that a dense/stiff collagen-I environment fostered the agonist activity of tamoxifen to increase proliferation and AP-1 activity in primary tumors. Manipulation of estrogen activity did not alter the incidence of lung lesions in either WT or mCol1a1 hosts. However, the mCol1a1 environment enabled tamoxifen-stimulated growth of pulmonary metastases and further fueled estrogen-driven growth. Moreover, estrogen remodeled peritumoral ECM architecture in WT animals, modifying alignment of collagen fibers and altering synthesis of ECM components. The lack of preclinical estrogen responsive, immunocompetent *in vivo* models of breast cancer has impeded our understanding of the breadth of mechanisms by which E2 and anti-estrogen therapeutics influence ER+ breast cancer. The *in vivo* studies presented here demonstrate the power of the ECM to dictate estrogen and anti-estrogen responses in ER+ breast cancer, and conversely, the influence of estrogen on this component of the tumor microenvironment (summarized in Suppl. Fig. 3).

ECM properties can markedly alter the activity of signaling pathways within tumor cells, increasing integrin-mediated activation of focal adhesion kinase and downstream kinases such as c-SRC, MAP kinases and AKT [1, 3, 28, 54]. Many of these signaling cascades regulate the expression and activity of AP-1 family members [42, 43, 55]. Dimers of AP-1 proteins alter transcription of target genes to drive multiple processes underlying cancer progression, including proliferation, anti-apoptosis, invasion, and angiogenesis [42, 43, 56, 57]. AP-1 activity also has been linked to ECM properties. The AP-1 protein, c-JUN, is upregulated in many fibrotic diseases, and forms a positive feedback loop with AKT [55]. Further, YAP-TAZ regulated TEAD factors, which are activated by mechanical signals [52, 58], synergize with AP-1 dimers to stimulate transcriptional enhancers [44]. Consistent with these relationships, the ER+ tumors in untreated mCol1a1 recipients in the current study exhibited elevated activity of these kinase cascades, and significantly higher nuclear c-JUN compared to primary tumors in WT recipients.

Importantly, AP-1 can also interact with the ER pathway. Activated ER tethered to AP-1 dimers can further upregulate their transcriptional activity [39–41]. Consistently, E2 augmented nuclear c-JUN and transcripts for AP-1 target genes in both WT and mCol1a1 recipients in our study. The ability of SERMs, including tamoxifen, to activate AP-1 in breast cancer cell lines *in vitro* has long been appreciated [59]. In multiple studies utilizing primarily MCF7-derived cell lines, increased AP-1 activity has been linked to reduced effectiveness of tamoxifen to inhibit growth [32–36], which also has been observed in some studies of patient tumors [34, 37, 38]. Growth factors activate many of the kinase cascades which drive this pathway, and elevated growth factor activity is also implicated in tamoxifen

resistance. Not surprisingly, the ER transcriptome in tamoxifen resistant experimental models and patient tumors overlaps with growth factor-regulated genes, and the promoters of many of these genes exhibit AP-1 binding sites [60, 61]. Our data demonstrate that the intensified kinase cascades in stiff/dense ECM, like those activated by growth factors, can strengthen tamoxifen-induced AP-1 activity, associated with heightened ER+ tumor aggression in an immunocompetent *in vivo* model.

Mammotropic hormones alter synthesis of ECM components [62, 63], and inhibition of estrogen action with tamoxifen alters the mammary ECM [64]. Involution of the mammary gland following weaning, which is associated with alterations in the balance of these hormones, is marked by changes in ECM composition and structure [65]. Our studies in the WT environment showed that elevated E2 substantially alters the ECM in the vicinity of the primary tumor. In contrast to tumors in untreated and tamoxifen-treated animals, which exhibited collagen fibers generally aligned parallel to the tumor edge (TACS-2) [45], tumors in E2-treated recipients exhibited many fibers oriented perpendicularly to the tumor boundary (TACS-3). In addition, E2 increased transcripts for COL1A1, matricellular components and the cross-linking enzyme, LOX, which increase ECM density and stiffness, and are clinically associated with aligned collagen fibers, tamoxifen resistance, and poor outcomes [47, 54, 66]. Further, E2 augmented *Tgfb1* transcripts, a key player in ECM remodeling and fibrosis [48, 67]. The E2-induced increase in FN1 expression in the primary and metastatic tumor environments, in combination with the recent report that fibronectin increases association of ER with integrin b1 [68], suggests one mechanism by which estrogen and the peritumoral ECM can positively feed forward to alter tumor behavior. Understanding how estrogen impacts the tumor microenvironment is critical. Prior to diagnosis, clinical cancers may be exposed to estrogen from the ovary in premenopausal women, and by locally produced estrogens in postmenopausal patients.

Interestingly, in the current study, manipulation of estrogen activity did not alter the number of lung metastases in either recipient genotype. In light of the E2-induced changes in the ECM composition and architecture, this was unexpected. Moreover, estrogen has been reported to promote cancer aggression by recruiting and activating immunosuppressive myeloid derived suppressor cells [69] and upregulating angiogenesis [70], even in non-breast (ER-) cancers. Notably, E2 treatment also did not increase lung metastases in the ER- MMTV-PyMT model [71]. In both the current and MMTV-PyMT study, E2 treatment was initiated after the primary tumors were established. However, tumor cells intravasate early in the disease process [72, 73], and circulating tumor cells peak 2.5–4 weeks after orthotopic transplantation of related murine ER+ cell lines [26]. It is therefore possible that tumor cells in the current study had disseminated and begun to colonize the lungs prior to the manipulation of estrogen activity. The relevance of timing of estrogen exposure on the steps in the metastatic cascade and identification of critical target cells deserve additional study.

Despite the failure to alter the frequency of lung metastases, E2 increased the size of pulmonary lesions in WT female recipients, which was further augmented in mCol1a1 females. In mCol1a1, but not WT recipients, tamoxifen also significantly increased the size of metastatic lesions, although not to the extent of E2. Interestingly, the number and size of the lung lesions that developed from tumor cells injected into tail veins did not differ

between the recipient genotypes, in marked contrast to the pulmonary metastases resulting from dissemination from the primary tumors. This suggests that the lungs of the WT and mCol1a1 mice do not exhibit substantial differences in attractiveness as potential metastatic sites. Instead, our data suggest that the increased E2- and tamoxifen-stimulated growth of lung metastases in the mCol1a1 model may be due to pulmonary seeding by more vigorous tumor cells nurtured in the stiffer environment of the primary tumor, or by more advantageous conditioning of the premetastatic niche in mCol1a1 mice. Future studies will dissect the mechanisms and mediators by which a stiff/dense ECM encourages the enhanced growth and estrogen/anti-estrogen responsiveness of lung metastases.

Metastasis, dormancy, and treatment resistance of ER+ breast cancer remain major clinical challenges. Our data demonstrate that a COL1A1-enriched fibrotic ECM, like elevated growth factor activity, strengthens kinase cascades, heightens AP-1 activity and permits tamoxifen agonism. The interplay of estrogen and SERMs with the ECM, and consequences for metastatic burden, highlight the importance of understanding the dynamic microenvironment of these cancers, in order to prevent and treat advanced disease.

Material and methods

Reagents

17β-estradiol (E2) (E2758) and tamoxifen citrate (T9272) were purchased from Sigma-Aldrich (St. Louis, MO, USA). Biotinylated goat anti-rabbit (BA-100), Avidin-biotin-complex (ABC) (PK-4000), ImmPACT DAB (SK-4105) were purchased from Vector Labs (Burlingame, CA, USA). Antibodies against the following proteins were purchased from these vendors: STAT5A (sc-1081), ERα (sc-542), Santa Cruz Biotechnology, Inc. (Santa Cruz, CA, USA); progesterone receptor (PR, A0098), Dako (Carpinteria, CA, USA); Ki-67 (ab15580), FN1 (ab23750), POSTN (ab14041), Abcam (Cambridge, MA, USA); c-JUN (cs 9165), PAK1 (cs 2602), pAKT S473 (cs 3787; cs9271), AKT (cs9272), pERK1/2 (cs 9101), ERK1/2 (cs9102), Cell Signaling Technology (Danvers, MA, USA), COL1A1 (NB600–450), Novus Biologicals, Centennial, CO, USA).

Animals and treatments

Heterozygous *Col1a1*^{tm1Jae} (*Col1a1*$^{tm1Jae/+}$, mCol1a1) mice were backcrossed onto the FVB/N strain background for more than 10 generations. Mice were housed and handled in accordance with the Guide for Care and Use of Laboratory Animals in AAALAC-accredited facilities, and all procedures were approved by the University of Wisconsin–Madison Animal Care and Use Committee. The TC11 cell line was generated from an ER+ mammary tumor that developed in a NRL-PRL female [19]. Like the parent tumors that develop spontaneously as a result of local transgenic prolactin overexpression in the mammary glands [18, 20], TC11 cells express low levels of progesterone receptor, but respond to E2 with robust proliferation and changes in gene expression [19]. For some of these studies, 10 000 TC11 cells in 50 μl of sterile PBS were orthotopically injected bilaterally into the caudal mammary fat pads of 10-week-old WT or mCol1a1 FVB/N female mice. When tumors were approximately 150 mm^3, mice from each genotype were randomly divided into 3 experimental groups: controls (unpelleted), E2 (20 μg)-pelleted, and tamoxifen (25 mg)-

pelleted. We used this low dose of E2, which delivers E2 to more physiologic levels in murine females, because of the bladder pathology associated with chronic treatment using higher doses [74, 75]. Sample sizes were based on power calculations using variability observed in similar studies. Animals were excluded only if they developed complications prior to end stage (n=1). Tumors were measured three times per week with calipers, and tumor volumes calculated (the largest diameter × (the smallest diameter)^2 × 0.4). When primary tumors reached end stage (1.5 cm in diameter), recipient mice were humanely euthanized and tissues collected. In order to distinguish effects on the early stages of metastasis from pulmonary colonization, 10 000 tumor cells were injected into the tail veins of WT and mCol1a1 females, and after 50 days, lungs were collected for analysis.

Immunohistochemistry/ Immunofluorescence

Immunohistochemistry analyses were performed as previously described [27] using the primary antibodies shown in Supplementary Table 1. Briefly, tissues were fixed in 10% neutral buffered formalin for 24 h, embedded in paraffin, and processed to 5μm sections. 10mM citrate buffer (pH 6.0) was used for antigen retrieval for all antibodies except PAK1, which required 10mM Tris buffer (pH 10). Signals were amplified by the avidin-biotin complex prior to chromogen detection with ImmPACT 3,3-diaminobenzidine and counter-staining with hematoxylin. Labeled cells were quantified by counting 200 cells in five random 40X fields of view (FOV).

Immunofluorescence analysis of the lungs and primary tumors was performed as previously described [76] with antibodies shown in Suppl. Table 1. Briefly, antigens were retrieved with citrate buffer. Following blocking, sections were subjected to the TSA Plus kit for tissue labeling following manufacturers' protocols (Perkin Elmer, fluorescein NEL741001KT and Cy 3.5 NEL763001KT, Waltham, MA), and were mounted in ProLong Gold with DAPI (Thermo Fisher Scientific P36931). Images were collected using a Nikon Eclipse TE300 inverted microscope with a Nikon Plan Fluor ELWD 20X/0.45 DIC L objective lens and an ORCA-R2 Digital CCD camera. A minimum of 6 images were collected from each lung section from 3 mice per treatment using SlideBook Software (v6) and processed using FIJI software. A mask was created of the tissue area and then applied to quantify the mean fluorescence intensity of FN1 or POSTN in each image. For all analyses, tissues were assessed and reported based on pathology numbers only, blinding investigators to treatments.

Immunoblotting

Relative levels of protein expression in individual tumors were determined by immunoblotting using the primary antibodies shown in Supplementary Table 1. Signals were detected by enhanced chemiluminescence and quantified by scanning densitometry (Vision WorksLS, v.7.1, UVP).

Quantitative real-time PCR

Tumor RNA was isolated, and specific transcripts were quantified by RT-PCR, normalized to 18S RNA, as described [27]. Primers utilized are shown in Suppl. Table 2.

Collagen imaging

Collagen fibers in paraffin sections were visualized by picrosirius red staining, as previously described [27, 77]. Signals were imaged using a Leica TSC SP8 Confocal Microscope (Wetzlar, Germany). Sample tissues were excited at 561 nm and emission was detected between 582 and 654 nm. LAS × software (Leica) was used to capture images at 512 × 512 resolution using z-stack. CT-fire software was used to detect fibers prior to analysis of fiber alignment, which was performed using CurveAlign software (LOCI; Madison, WI) [78]. Collagen fibers in at least five random 63x FOVs for each tumor were analyzed.

Analysis of lung metastases

Lung metastases were analyzed as previously described [26]. Briefly, at end stage following orthotopic transplantation or 50 days after tail vein injection, lungs were collected and processed for sections, which were stained with hematoxylin and eosin. For lungs from animals with orthotopic tumors, lesions detectable in 5 random 4x FOV were assessed. For lungs of animals following tail vein injections, the lung lesions detectable at 4x were counted over the entire section, normalized for section area. The sizes of all metastases lesions were calculated using ImageJ software.

Statistical analysis

Statistical analyses were performed using GraphPad Prism v.7 (GraphPad software, Inc. San Diego, CA), utilizing the tests noted in the figure legends. Similar variance was observed in statistically compared groups. Differences were considered significant at $P<0.05$.

Supplementary Material

Refer to Web version on PubMed Central for supplementary material.

Acknowledgements

We would like to thank Kyle Wegner for assistance with picrosirius red staining and image processing, and Ashley Weichmann in the UW Carbone Cancer Center Small Animal Imaging Facility for assistance with the tail vein injections. We are grateful to Dr. Elaine Alarid for helpful discussions.

Funding:

This work was supported by the National Institutes of Health [R01 CA157675 (LAS) and R01 CA179556 (LAS, SMP), T32 HD041921 and R25 GM083252 (FJ), P30CA014520 (University of Wisconsin Carbone Cancer Center)], and funds from the UWCCC Breast Disease Oriented Team.

References

1. Keely PJ. Mechanisms by which the extracellular matrix and integrin signaling act to regulate the switch between tumor suppression and tumor promotion. J Mammary Gland Biol Neoplasia 2011; 16:205–219. [PubMed: 21822945]
2. Cox TR, Erler JT. Molecular pathways: connecting fibrosis and solid tumor metastasis. Clin Cancer Res 2014; 20:3637–3643. [PubMed: 25028505]
3. Kaushik S, Pickup MW, Weaver VM. From transformation to metastasis: deconstructing the extracellular matrix in breast cancer. Cancer Metastasis Rev 2016; 35:655–667. [PubMed: 27914000]

4. Robertson C The extracellular matrix in breast cancer predicts prognosis through composition, splicing, and crosslinking. Exp Cell Res 2016; 343:73–81. [PubMed: 26597760]
5. Al-Adnani MS, Kirrane JA, McGee JO. Inappropriate production of collagen and prolyl hydroxylase by human breast cancer cells in vivo. Br J Cancer 1975; 31:653–660. [PubMed: 169865]
6. Walker RA. The complexities of breast cancer desmoplasia. Breast Cancer Res 2001; 3:143–145. [PubMed: 11305947]
7. Anderson WF, Katki HA, Rosenberg PS. Incidence of breast cancer in the United States: current and future trends. J Natl Cancer Inst 2011; 103:1397–1402. [PubMed: 21753181]
8. Conklin MW, Eickhoff JC, Riching KM, Pehlke CA, Eliceiri KW, Provenzano PP, et al. Aligned collagen is a prognostic signature for survival in human breast carcinoma. Am J Pathol 2011; 178:1221–1232. [PubMed: 21356373]
9. Nardone A, De Angelis C, Trivedi MV, Osborne CK, Schiff R. The changing role of ER in endocrine resistance. Breast 2015; 24 Suppl 2:S60–66. [PubMed: 26271713]
10. Nagaraj G, Ma C. Revisiting the estrogen receptor pathway and its role in endocrine therapy for postmenopausal women with estrogen receptor-positive metastatic breast cancer. Breast Cancer Res Treat 2015; 150:231–242. [PubMed: 25762475]
11. Pan H, Gray R, Braybrooke J, Davies C, Taylor C, McGale P, et al. 20-Year Risks of breast-cancer recurrence after stopping endocrine therapy at 5 Years. New Engl J Med 2017; 377:1836–1846. [PubMed: 29117498]
12. Byrne C, Ursin G, Martin CF, Peck JD, Cole EB, Zeng D, et al. Mammographic density change with estrogen and progestin therapy and breast cancer risk. J Natl Cancer Inst 2017; 109:
13. Bertrand KA, Eliassen AH, Hankinson SE, Rosner BA, Tamimi RM. Circulating hormones and mammographic density in premenopausal women. Horm Cancer 2018; 9:117–127. [PubMed: 29330698]
14. Barcus CE, Keely, P.J., Eliceiri, K.W. and Schuler, L.A. Stiff collagen matrices increase tumorigenic prolactin signaling in breast cancer cells. J Biol Chem 2013; 288:12722–12732. [PubMed: 23530035]
15. Barcus CE, Holt EC, Keely PJ, Eliceiri KW, Schuler LA. Dense collagen-I matrices enhance pro-tumorigenic estrogen-prolactin crosstalk in MCF-7 and T47D breast cancer cells. PloS one 2015; 10:e0116891. [PubMed: 25607819]
16. Barcus CE, Keely PJ, Eliceiri KW, Schuler LA. Prolactin signaling through focal adhesion complexes is amplified by stiff extracellular matrices in breast cancer cells. Oncotarget 2016; 7:48093–48106. [PubMed: 27344177]
17. Burstein HJ, Temin S, Anderson H, Buchholz TA, Davidson NE, Gelmon KE, et al. Adjuvant endocrine therapy for women with hormone receptor-positive breast cancer: american society of clinical oncology clinical practice guideline focused update. J Clin Oncol 2014; 32:2255–2269. [PubMed: 24868023]
18. O'Leary KA, Shea MP, Schuler LA. Modeling prolactin actions in breast cancer in vivo: insights from the NRL-PRL mouse. Adv Exp Med Biol 2015; 846:201–220. [PubMed: 25472540]
19. Jallow F, Brockman JL, Helzer KT, Rugowski DE, Goffin V, Alarid ET, et al. 17beta-Estradiol and ICI182,780 differentially regulate STAT5 isoforms in female mammary epithelium, with distinct outcomes. J Endoc Soc 2018; 2:293–309.
20. Campbell KM, O'Leary KA, Rugowski DE, Mulligan WA, Barnell EK, Skidmore ZL, et al. Spontaneous aggressive ERα+ mammary tumor model is driven by Kras activation. Cell Reports, in press.
21. Liu X, Wu H, Byrne M, Jeffrey J, Krane S, Jaenisch R. A targeted mutation at the known collagenase cleavage site in mouse type I collagen impairs tissue remodeling. J Cell Biol 1995; 130:227–237. [PubMed: 7790374]
22. Smid M, Wang Y, Zhang Y, Sieuwerts AM, Yu J, Klijn JG, et al. Subtypes of breast cancer show preferential site of relapse. Cancer Res 2008; 68:3108–3114. [PubMed: 18451135]
23. Kennecke H, Yerushalmi R, Woods R, Cheang MC, Voduc D, Speers CH, et al. Metastatic behavior of breast cancer subtypes. J Clin Oncol 2010; 28:3271–3277. [PubMed: 20498394]

24. Molnar IA, Molnar BA, Vizkeleti L, Fekete K, Tamas J, Deak P, et al. Breast carcinoma subtypes show different patterns of metastatic behavior. Virchows Archiv 2017; 470:275–283. [PubMed: 28101678]
25. Provenzano PP, Inman DR, Eliceiri KW, Knittel JG, Yan L, Rueden CT, et al. Collagen density promotes mammary tumor initiation and progression. BMC Med 2008; 6:11. [PubMed: 18442412]
26. Barcus CE, O'Leary KA, Brockman JL, Rugowski DE, Liu Y, Garcia N, et al. Elevated collagen-I augments tumor progressive signals, intravasation and metastasis of prolactin-induced estrogen receptor alpha positive mammary tumor cells. Breast Cancer Res 2017; 19:9. [PubMed: 28103936]
27. Shea MP, O'Leary KA, Wegner KA, Vezina CM, Schuler LA. High collagen density augments mTOR-dependent cancer stem cells in ERα+ mammary carcinomas, and increases mTOR-independent lung metastases. Cancer Lett 2018; 433:1–9. [PubMed: 29935374]
28. Zanconato F, Cordenonsi M, Piccolo S. YAP/TAZ at the roots of cancer. Cancer Cell 2016; 29:783–803. [PubMed: 27300434]
29. Kumar R, Gururaj AE, Barnes CJ. p21-activated kinases in cancer. Nat Rev Cancer 2006; 6:459–471. [PubMed: 16723992]
30. Holm C, Rayala S, Jirstrom K, Stal O, Kumar R, Landberg G. Association between Pak1 expression and subcellular localization and tamoxifen resistance in breast cancer patients. J Natl Cancer Inst 2006; 98:671–680. [PubMed: 16705121]
31. Ong CC, Jubb AM, Haverty PM, Zhou W, Tran V, Truong T, et al. Targeting p21-activated kinase 1 (PAK1) to induce apoptosis of tumor cells. Proc Natl Acad Sci U S A 2011; 108:7177–7182. [PubMed: 21482786]
32. Dumont JA, Bitonti AJ, Wallace CD, Baumann RJ, Cashman EA, Cross-Doersen DE. Progression of MCF-7 breast cancer cells to antiestrogen-resistant phenotype is accompanied by elevated levels of AP-1 DNA-binding activity. Cell Growth Differ 1996; 7:351–359. [PubMed: 8838865]
33. Smith LM, Wise SC, Hendricks DT, Sabichi AL, Bos T, Reddy P, et al. cJun overexpression in MCF-7 breast cancer cells produces a tumorigenic, invasive and hormone resistant phenotype. Oncogene 1999; 18:6063–6070. [PubMed: 10557095]
34. Zhou Y, Yau C, Gray JW, Chew K, Dairkee SH, Moore DH, et al. Enhanced NF kappa B and AP-1 transcriptional activity associated with antiestrogen resistant breast cancer. BMC Cancer 2007; 7:59. [PubMed: 17407600]
35. Malorni L, Giuliano M, Migliaccio I, Wang T, Creighton CJ, Lupien M, et al. Blockade of AP-1 potentiates endocrine therapy and overcomes resistance. Mol Cancer Res 2016; 14:470–481. [PubMed: 26965145]
36. He H, Sinha I, Fan R, Haldosen LA, Yan F, Zhao C, et al. c-Jun/AP-1 overexpression reprograms ERα signaling related to tamoxifen response in ERα-positive breast cancer. Oncogene 2018; 37:2586–2600. [PubMed: 29467493]
37. Johnston SR, Lu B, Scott GK, Kushner PJ, Smith IE, Dowsett M, et al. Increased activator protein-1 DNA binding and c-Jun NH2-terminal kinase activity in human breast tumors with acquired tamoxifen resistance. Clin Cancer Res 1999; 5:251–256. [PubMed: 10037172]
38. Insua-Rodriguez J, Pein M, Hongu T, Meier J, Descot A, Lowy CM, et al. Stress signaling in breast cancer cells induces matrix components that promote chemoresistant metastasis. EMBO Mol Med 2018; 10:
39. Kushner PJ, Agard DA, Greene GL, Scanlan TS, Shiau AK, Uht RM, et al. Estrogen receptor pathways to AP-1. J Steroid Biochem Mol Biol 2000; 74:311–317. [PubMed: 11162939]
40. Jakacka M, Ito M, Weiss J, Chien PY, Gehm BD, Jameson JL. Estrogen receptor binding to DNA is not required for its activity through the nonclassical AP1 pathway. J Biol Chem 2001; 276:13615–13621. [PubMed: 11278408]
41. Cheung E, Acevedo ML, Cole PA, Kraus WL. Altered pharmacology and distinct coactivator usage for estrogen receptor-dependent transcription through activating protein-1. Proc Natl Acad Sci USA 2005; 102:559–564. [PubMed: 15642950]
42. Shaulian E, Karin M. AP-1 as a regulator of cell life and death1. Nat Cell Biol 2002; 4:E131–E136. [PubMed: 11988758]
43. Eferl R, Wagner EF. AP-1: a double-edged sword in tumorigenesis. Nat Rev Cancer 2003; 3:859–868. [PubMed: 14668816]

44. Zanconato F, Forcato M, Battilana G, Azzolin L, Quaranta E, Bodega B, et al. Genome-wide association between YAP/TAZ/TEAD and AP-1 at enhancers drives oncogenic growth. Nat Cell Biol 2015; 17:1218–1227. [PubMed: 26258633]
45. Provenzano PP, Eliceiri KW, Campbell JM, Inman DR, White JG, Keely PJ. Collagen reorganization at the tumor-stromal interface facilitates local invasion. BMC Med 2006; 4:38. [PubMed: 17190588]
46. Houthuijzen JM, Jonkers J. Cancer-associated fibroblasts as key regulators of the breast cancer tumor microenvironment. Cancer Metas Rev 2018;
47. Tomko LA, Hill RC, Barrett A, Szulczewski JM, Conklin MW, Eliceiri KW, et al. Targeted matrisome analysis identifies thrombospondin-2 and tenascin-C in aligned collagen stroma from invasive breast carcinoma. Sci Reports 2018; 8:12941.
48. Gyorfi AH, Matei AE, Distler JHW. Targeting TGF-beta signaling for the treatment of fibrosis. Matrix Biol 2018; 68–69:8–27.
49. Socovich AM, Naba A. The cancer matrisome: From comprehensive characterization to biomarker discovery. Sem Cell Dev Biol 2019; 89:157–166.
50. Kaplan RN, Riba RD, Zacharoulis S, Bramley AH, Vincent L, Costa C, et al. VEGFR1-positive haematopoietic bone marrow progenitors initiate the pre-metastatic niche. Nature 2005; 438:820–827. [PubMed: 16341007]
51. Oskarsson T, Acharyya S, Zhang XH, Vanharanta S, Tavazoie SF, Morris PG, et al. Breast cancer cells produce tenascin C as a metastatic niche component to colonize the lungs. Nat Med 2011; 17:867–874. [PubMed: 21706029]
52. Moroishi T, Hansen CG, Guan KL. The emerging roles of YAP and TAZ in cancer. Nat Rev Cancer 2015; 15:73–79. [PubMed: 25592648]
53. Evans A, Sim YT, Pourreyron C, Thompson A, Jordan L, Fleming D, et al. Pre-operative stromal stiffness measured by shear wave elastography is independently associated with breast cancer-specific survival. Breast Cancer Res Treat 2018; 171:383–389. [PubMed: 29858751]
54. Pontiggia O, Sampayo R, Raffo D, Motter A, Xu R, Bissell MJ, et al. The tumor microenvironment modulates tamoxifen resistance in breast cancer: a role for soluble stromal factors and fibronectin through beta1 integrin. Breast Cancer Res Treat 2012; 133:459–471. [PubMed: 21935603]
55. Wernig G, Chen SY, Cui L, Van Neste C, Tsai JM, Kambham N, et al. Unifying mechanism for different fibrotic diseases. Proc Natl Acad Sci U S A 2017; 114:4757–4762. [PubMed: 28424250]
56. Clark IM, Swingler TE, Sampieri CL, Edwards DR. The regulation of matrix metalloproteinases and their inhibitors. Int J Biochem Cell Biol 2008; 40:1362–1378. [PubMed: 18258475]
57. Shen Q, Uray IP, Li Y, Krisko TI, Strecker TE, Kim HT, et al. The AP-1 transcription factor regulates breast cancer cell growth via cyclins and E2F factors. Oncogene 2008; 27:366–377. [PubMed: 17637753]
58. Dupont S Role of YAP/TAZ in cell-matrix adhesion-mediated signalling and mechanotransduction. Exp Cell Res 2016; 343:42–53. [PubMed: 26524510]
59. Webb P, Lopez GN, Uht RM, Kushner PJ. Tamoxifen activation of the estrogen receptor/AP-1 pathway: potential origin for the cell-specific estrogen-like effects of antiestrogens. Mol Endocrinol 1995; 9:443–456. [PubMed: 7659088]
60. Lupien M, Meyer CA, Bailey ST, Eeckhoute J, Cook J, Westerling T, et al. Growth factor stimulation induces a distinct ER(alpha) cistrome underlying breast cancer endocrine resistance. Genes Dev 2010; 24:2219–2227. [PubMed: 20889718]
61. Massarweh S, Osborne CK, Creighton CJ, Qin L, Tsimelzon A, Huang S, et al. Tamoxifen resistance in breast tumors is driven by growth factor receptor signaling with repression of classic estrogen receptor genomic function. Cancer Res 2008; 68:826–833. [PubMed: 18245484]
62. Haslam SZ, Woodward TL. Reciprocal regulation of extracellular matrix proteins and ovarian steroid activity in the mammary gland. Breast Cancer Res 2001; 3:365–372. [PubMed: 11737887]
63. Calvo E, Luu-The V, Belleau P, Martel C, Labrie F. Specific transcriptional response of four blockers of estrogen receptors on estradiol-modulated genes in the mouse mammary gland. Breast Cancer Res Treat 2012; 134:625–647. [PubMed: 22678160]

64. Hattar R, Maller O, McDaniel S, Hansen KC, Hedman KJ, Lyons TR, et al. Tamoxifen induces pleiotrophic changes in mammary stroma resulting in extracellular matrix that suppresses transformed phenotypes. Breast Cancer Res 2009; 11:R5. [PubMed: 19173736]

65. Goddard ET, Hill RC, Nemkov T, D'Alessandro A, Hansen KC, Maller O, et al. The rodent liver undergoes weaning-Induced involution and supports breast cancer metastasis. Cancer Disc 2017; 7:177–187.

66. Helleman J, Jansen MP, Ruigrok-Ritstier K, Van Staveren IL, Look MP, Meijer-van Gelder ME, et al. Association of an extracellular matrix gene cluster with breast cancer prognosis and endocrine therapy response. Clin Cancer Res 2008; 14:5555–5564. [PubMed: 18765548]

67. Kim KK, Sheppard D, Chapman HA. TGF-beta1 signaling and tissue fibrosis. Cold Spring Harbor Perspec Biol 2018; 10:

68. Sampayo RG, Toscani AM, Rubashkin MG, Thi K, Masullo LA, Violi IL, et al. Fibronectin rescues estrogen receptor alpha from lysosomal degradation in breast cancer cells. J Cell Biol 2018; 217:2777–2798. [PubMed: 29980625]

69. Svoronos N, Perales-Puchalt A, Allegrezza MJ, Rutkowski MR, Payne KK, Tesone AJ, et al. Tumor cell-independent estrogen signaling drives disease progression through mobilization of myeloid-derived suppressor cells. Cancer Disc 2017; 7:72–85.

70. Dabrosin C, Margetts PJ, Gauldie J. Estradiol increases extracellular levels of vascular endothelial growth factor in vivo in murine mammary cancer. Int J Cancer 2003; 107:535–540. [PubMed: 14520689]

71. Nelson ER, Wardell SE, Jasper JS, Park S, Suchindran S, Howe MK, et al. 27-Hydroxycholesterol links hypercholesterolemia and breast cancer pathophysiology. Science 2013; 342:1094–1098. [PubMed: 24288332]

72. Klein CA. Parallel progression of primary tumours and metastases. Nat Rev Cancer 2009; 9:302–312. [PubMed: 19308069]

73. Valastyan S, Weinberg RA. Tumor metastasis: molecular insights and evolving paradigms. Cell 2011; 147:275–292. [PubMed: 22000009]

74. Kang JS, Kang MR, Han SB, Yoon WK, Kim JH, Lee TC, et al. Low dose estrogen supplementation reduces mortality of mice in estrogen-dependent human tumor xenograft model. Biol Pharm Bull 2009; 32:150–152. [PubMed: 19122299]

75. Gerard C, Gallez A, Dubois C, Drion P, Delahaut P, Quertemont E, Noel A, et al. Accurate control of 17beta-estradiol long-term release increases reliability and reproducibility of preclinical animal studies. J Mammary Gland Biol Neoplasia 2017; 22:1–11. [PubMed: 27889857]

76. Esbona K, Yi Y, Saha S, Yu M, Van Doorn RR, Conklin MW, et al. The presence of cyclooxygenase 2, tumor-associated macrophages, and collagen alignment as prognostic markers for invasive breast carcinoma patients. Am J Pathol 2018; 188:559–573. [PubMed: 29429545]

77. Wegner KA, Keikhosravi A, Eliceiri KW, Vezina CM. Fluorescence of picrosirius red multiplexed with immunohistochemistry for the quantitative assessment of collagen in tissue sections. J Histochem Cytochem 2017; 65:479–490. [PubMed: 28692327]

78. Liu Y, Keikhosravi A, Mehta GS, Drifka CR, Eliceiri KW. Methods for quantifying fibrillar collagen alignment. Methods Mol Biol 2017; 1627:429–451. [PubMed: 28836218]

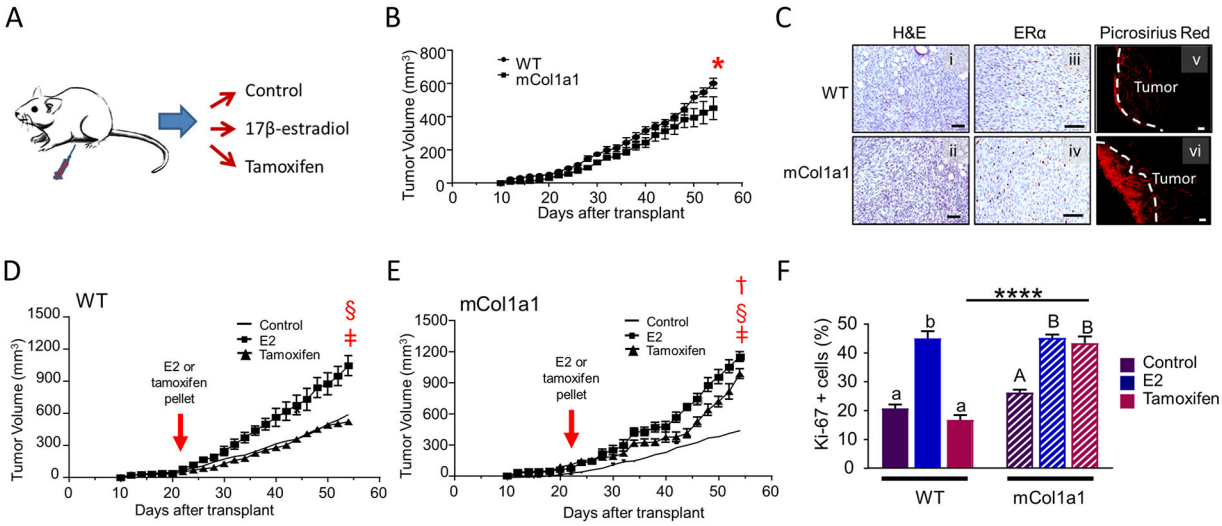

Fig. 1.

Primary tumors are estrogen responsive, and both E2 and tamoxifen increase tumor growth in mCol1a1 recipients**. a** Experimental design. TC11 cells were orthotopically transplanted into WT and mCol1a1 recipients. When tumors reached 150 mm^3 (21 – 23 days post-transplantation), the estrogen environment was modulated by administration of E2 or tamoxifen, or no treatment, as described in the Materials and methods. Tumor volumes were measured three times per week, and tissues were collected when primary tumors reached end-stage. **b** Primary tumors grew faster in wildtype (WT) than in mCol1a1 recipients. (Mean ± SEM; n=12). Significant interaction with genotype, determined by repeated measures two-way ANOVA, $*p = 0.03$. **c** Collagen environment did not alter morphology (i, ii; hematoxylin and eosin, H&E), or ER expression assessed by immunohistochemistry (iii, iv). Picrosirius red staining (v-vi) demonstrated accumulated fibrillar collagen around boundaries of primary tumors in mCol1a1 recipients. Original magnifications, x200; scale bars, 50 μm. **d, e** Tumor growth curves show that 17β-estradiol (E2) increased tumor growth in both recipient genotypes (**d,e**) and tamoxifen increased tumor growth in the mCol1a1 females (**e**). Solid lines depict mean sizes of primary tumors in untreated animals from (**b**). (Mean ± SEM; n=10–14). (**b,d,e**), Significant differences in tumor volumes between genotypes and among treatment groups were determined by repeated measures two-way ANOVA. ‡ denotes a significant difference between control and E2, $p < 0.0001$; † denotes a significant difference between control and tamoxifen-treated animals, $p < 0.0001$; § denotes a significant difference between E2- and tamoxifen-treated animals, $p < 0.0001$. **f** Rate of proliferation of tumor cells at the time of collection, assessed by nuclear Ki-67 staining. (Mean ± SEM; n= 5). Significant differences were determined by two-way ANOVA, followed by the Bonferroni post-test. Lower case letters denote significant differences with treatment in WT recipients, and uppercase letters denote significant differences with treatment in mCol1a1 recipients ($p < 0.0001$). **** denotes a significant difference between recipient genotypes administered the same treatment ($p < 0.0001$).

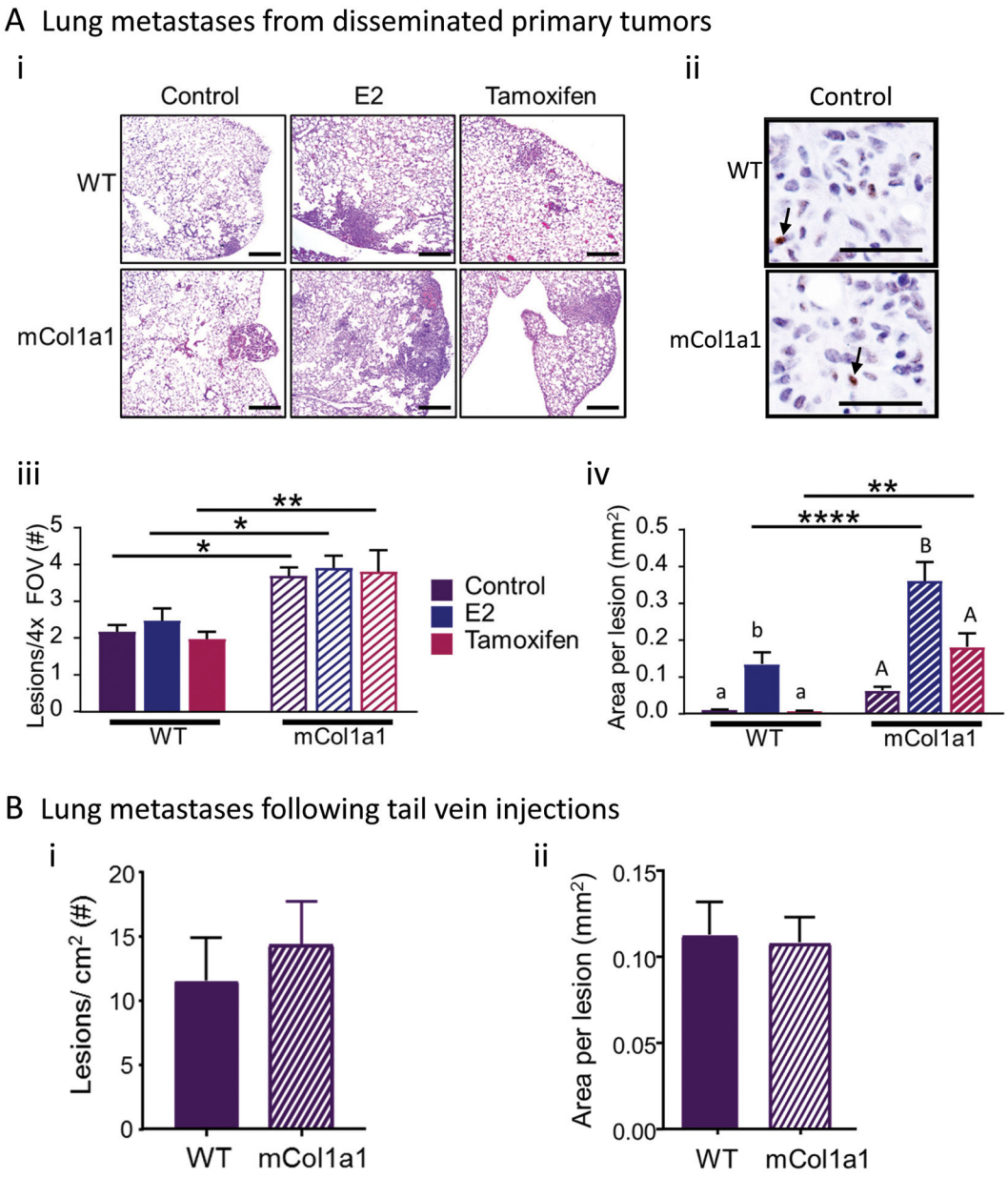

Fig. 2.

a mCol1a1 recipients develop more lung metastases, and 17β-estradiol (E2) significantly increases the size of lung metastases. **i** Photomicrographs of lung metastases (H&E) from recipients of orthotopic transplants treated as shown. Original magnifications, x40; scale bars, 500 μm. **ii** ER immunohistochemistry. Arrows point to ER+ metastatic cells. Original magnifications, x200; scale bars, 50 μm. **iii** Number of lesions per 4x field of view (FOV). **iv** Area of individual lesions. **b** Lungs of WT and mCol1a1 females which had been injected with 10 000 tumor cells into their tail veins displayed similar numbers (**i**) and sizes (**ii**) of lung lesions after 50 days. (Mean ± SEM; n=4–6 mice). Significant differences were determined by two-way ANOVA, followed by the Bonferroni post-test. Lower case letters denote significant differences with treatment in WT recipients and uppercase letters denote

significant differences in mCol1a1 recipients ($p < 0.02$). * denotes significant differences between recipient genotypes (*$p < 0.05$, **$p < 0.01$, ****$p < 0.0001$).

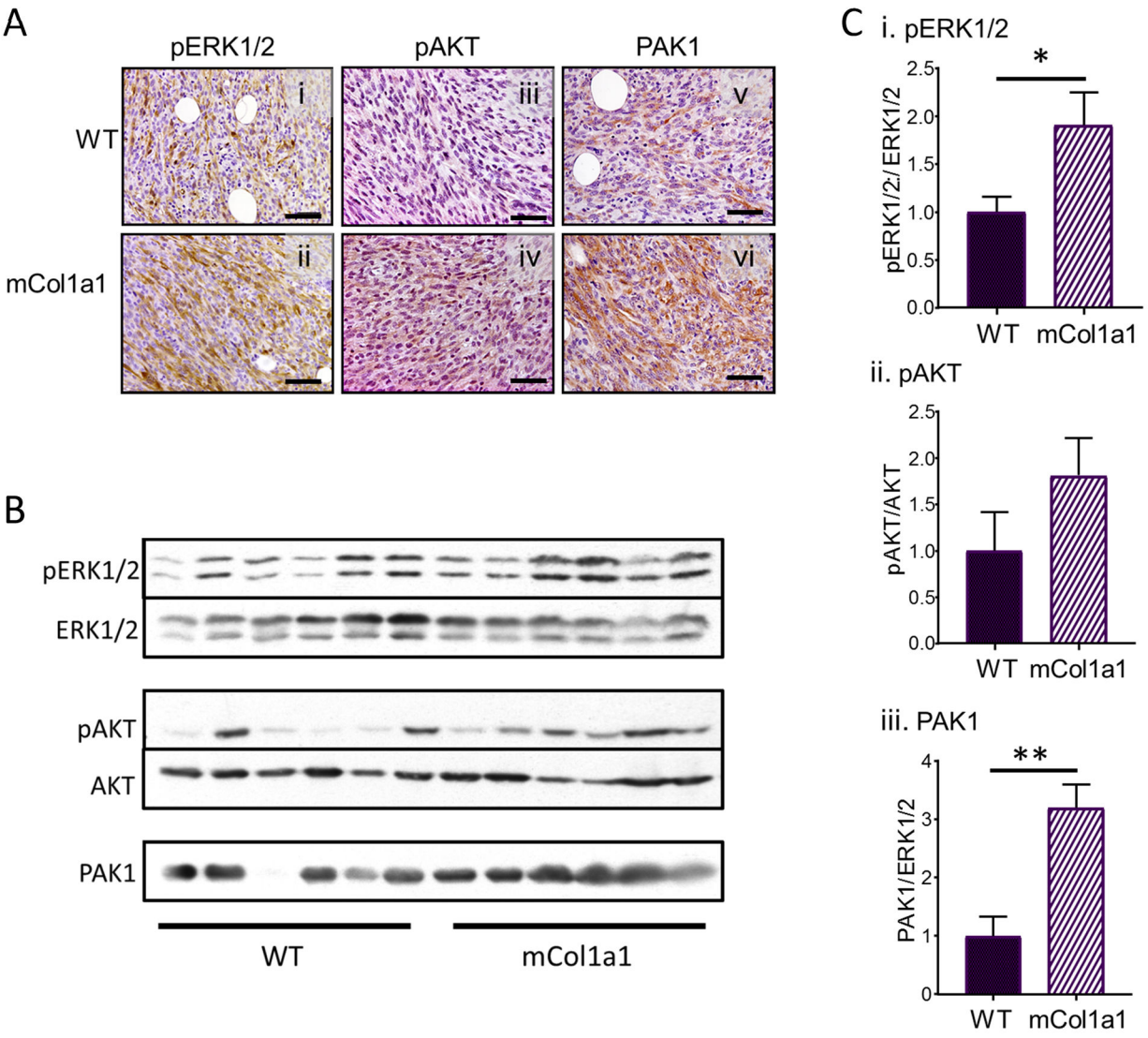

Fig. 3.

Primary tumors in mCol1a1 recipients exhibit higher activation of oncogenic signaling pathways. **a** Immunohistochemistry of primary tumors for pERK (i, ii), pAKT (iii, iv), and total PAK1 (v, vi). Original magnifications, x200; scale bars, 50 μm. **b** Tumor lysates were immunoblotted for the proteins shown. **c** Quantification of the signals in (b) as shown. (Mean ± SEM, n=6). Significant differences were determined by unpaired Students t test (*$p < 0.05$, **$p < 0.002$).

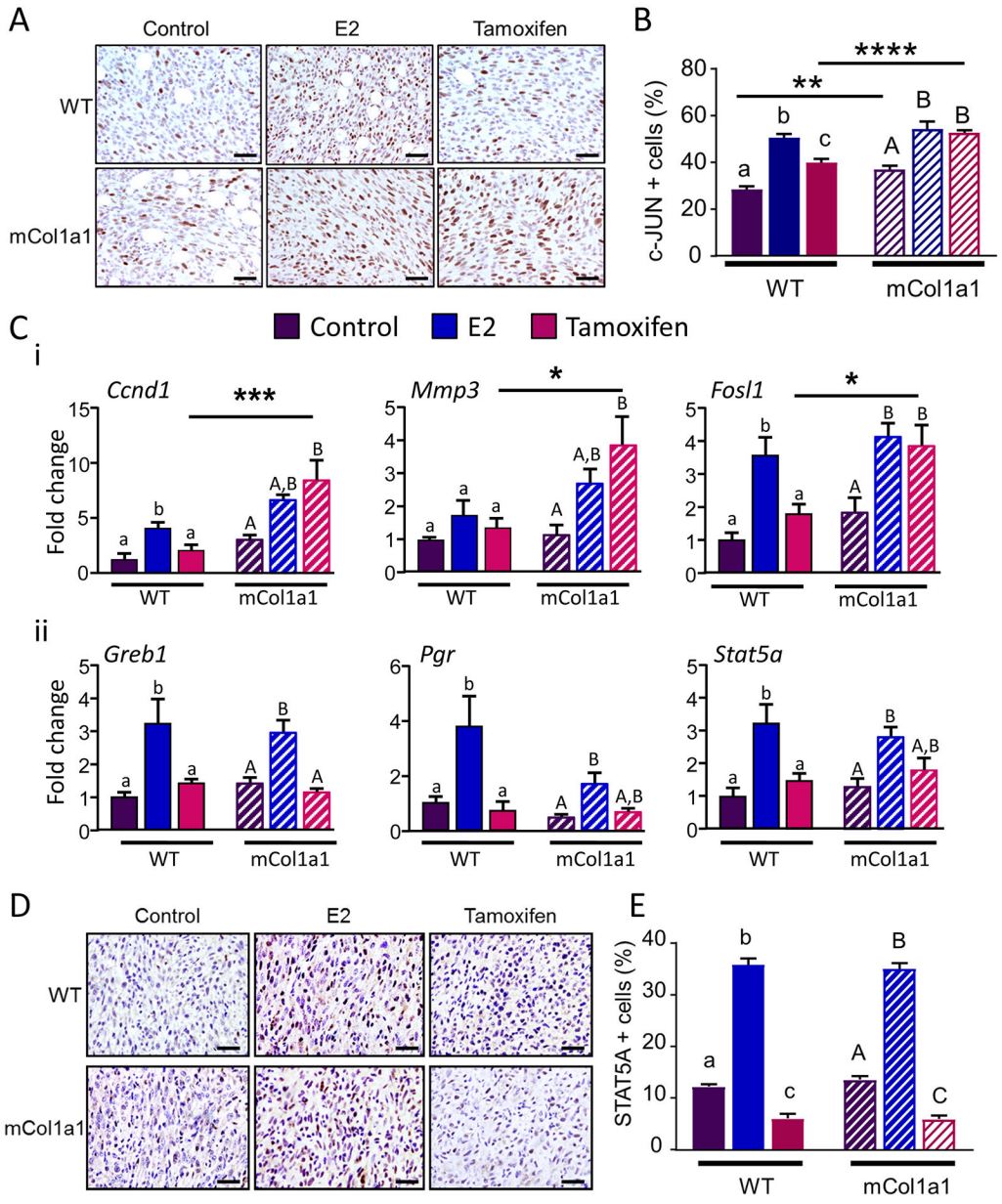

Fig. 4.

Collagen 1-rich environments activate AP-1. **a** Representative c-JUN immunohistochemistry in primary tumors in recipients of different genotypes and treatments. **b** Quantification of the proportion of tumor cells exhibiting nuclear c-JUN staining. **c i** Relative levels of transcripts for AP-1 regulated genes in primary tumors in recipients of different genotypes and treatments determined by RT-PCR, normalized to 18S RNA. **ii** Relative levels of transcripts for ERE-regulated genes in primary tumors in recipients of different genotypes and treatments determined by RT-PCR, normalized to 18S RNA. **d** Representative STAT5A immunohistochemistry in primary tumors in recipients of different genotypes and treatments. **f** Quantification of the proportion of tumor cells exhibiting nuclear STAT5A staining. **a, d** Original magnifications, x200; scale bars, 50 μm. **b, c, e**. Mean ± SEM; n=4–6.

Significant differences with treatment were determined by one-way ANOVA, followed by the Bonferroni post-test. Lower case letters denote significant differences with treatment in WT recipients and uppercase letters denote significant differences in mCol1a1 recipients ($p < 0.05$). Significant differences between genotypes with the same treatment were determined by two-way ANOVA, followed by the Bonferroni post-test. * denotes significant differences between recipient genotypes (*$p < 0.05$, **$p < 0.01$, ***$p < 0.001$, ****$p < 0.0001$).

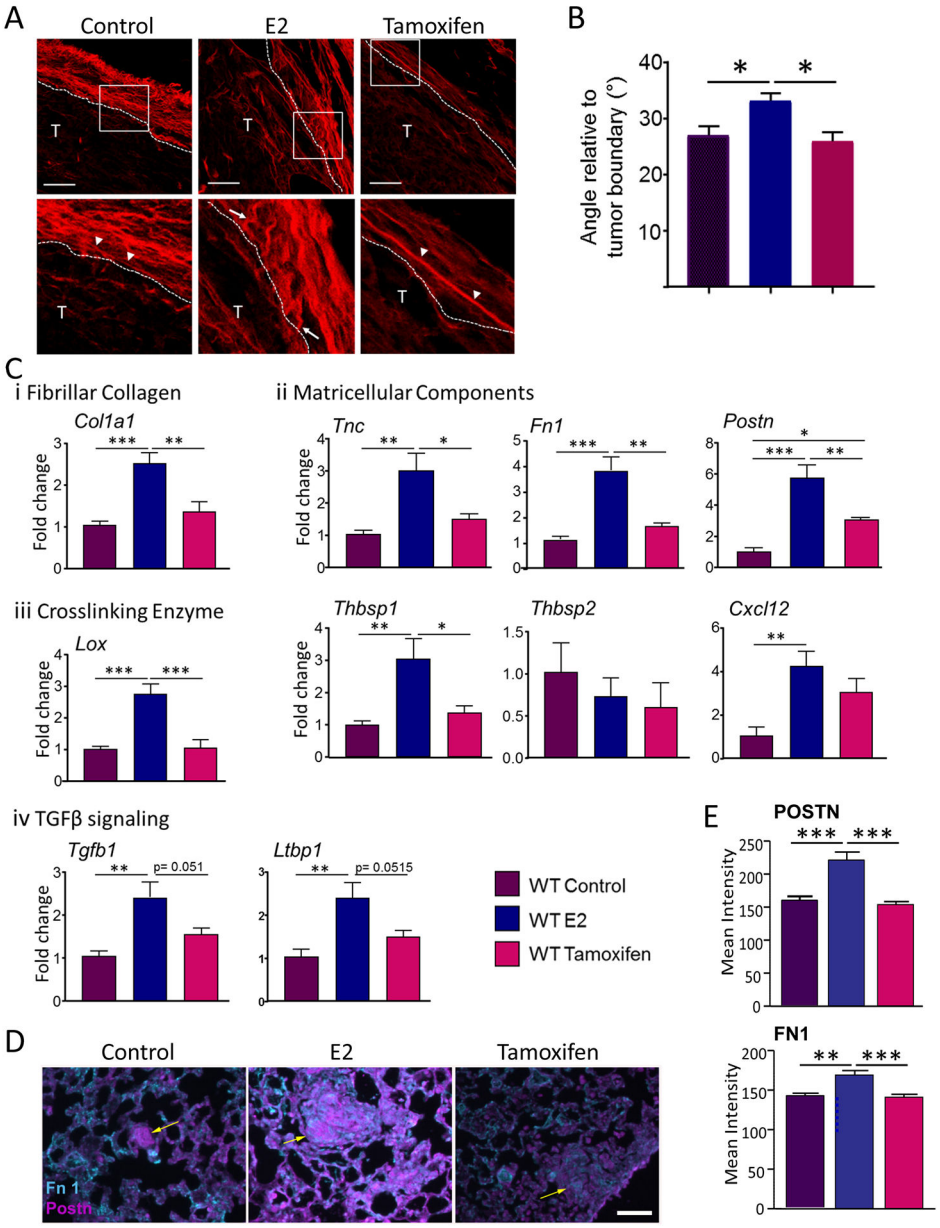

Fig. 5.

Estrogen activity modulates components of the ECM in the tumor microenvironment. **a** Picrosirius red-stained fibrillar collagens at the tumor boundary in WT females, treated as shown. Dotted line denotes the tumor boundary; T = tumor. White box in the top panel denotes the region enlarged in the lower panel. Arrowheads point to fibers aligned parallel to the tumor boundary (TACS-2), prominent in untreated and tamoxifen treated females, and arrows point to fibers perpendicular to the tumor boundary (TACS-3), enriched in E2-treated animals. Original magnifications x630; scale bars, 30 μm. **b** Angles of collagen fibers relative to the tumor boundary were calculated using CurveAlign (see Materials and methods). Mean ± SEM; n= 4–5. **c** Transcripts for ECM components determined by RT-PCR, normalized to 18S RNA. Mean ± SEM; n= 4–5. Significant differences were

determined by one-way ANOVA, followed by Tukey's post-test. * denotes significant differences between recipient genotypes (*$p < 0.05$, **$p < 0.01$, ***$p < 0.001$). **d** Representative pseudo-colored immunofluorescent images of expression of the matricellular proteins, FN1 and POSTN, in lung sections from control, E2- or tamoxifen-treated WT mice. Arrow indicates the metastatic lesion. Original magnifications, x200; scale bar, 50μm. **e** Quantification of POSTN and FN1 fluorescence was determined as described in the Methods. (Mean ± SEM; n=3 mice per group). Significant differences were determined by Dunn's multiple comparison test. * denotes significant differences between treatment groups (** $p < 0.01$, *** $p < 0.001$).